III European Conference on Computational Mechanics
Solids, Structures and Coupled Problems in Engineering
C.A. Mota Soares et.al. (eds.)
Lisbon, Portugal, 5–8 June 2006

STRAIN LOCALIZATION ANALYSIS USING LARGE DEFORMATION ANISOTROPIC ELASTOPLASTIC MODEL COUPLED WITH DAMAGE

Badis Haddag[1], **Farid Abed-Meraim**[1] **and Tudor Balan**[1]

[1] LPMM, CNRS UMR 7554, ENSAM Metz
4 rue A. Fresnel, 57078 Metz Cedex 3, France
e-mail: {badis.haddag,farid.abed-meraim,tudor.balan}@metz.ensam.fr

Keywords: Strain Localization, Anisotropic Elastoplasticity, Large Strain, Isotropic-Kinematic Hardening, Continuum Damage Theory, Shear Band, Finite Element Simulation.

Abstract. *This work aims to study the strain localization during the plastic deformation of sheets metals. This phenomenon is precursor for the fracture of drawing parts, so its prediction using advanced behavior models is an active research field. Most often, an accurate prediction of localization requires damage to be considered in the simulation.*

For this purpose, an advanced, anisotropic elastoplastic model has been coupled with a classical, isotropic damage model. The coupling with the damage model is carried out in the frame of continuum damage mechanics. In order to detect the localization during sheet forming, Rice's localization criterion is introduced.

The coupled elastoplastic damage model is implemented in the Abaqus/Implicit software, via the user routine UMAT, while Rice's criterion is incorporated in the same code, via the user routine UVARM. Simulations of typical rheological tests are performed in the numerical investigation. The predicted forming limits are very consistent with literature results. The fully 3D formulation adopted in our development allowed for some new results – like the out-of-plane orientation of the normal to the localization band.

1 INTRODUCTION

The numerical prediction of the metal forming defects is a constant preoccupation both for scientists and industry. The strain localization in sheet metal forming is usually assessed in terms of the so-called forming limit diagram [1]. During the last century, numerous criteria of localization have been proposed, e.g. maximum of the load [2, 3], Hill's bifurcation analysis [4], or models assuming an initial defect in the material [5]. One important way to improve the predictability of these models is clearly their coupling with an accurate constitutive model, eventually including damage. The more pragmatic models (e.g. the Marciniak-Kuczynski model) have been paid extensive attention in this direction, due to their industrial applications, in spite of their weaker theoretical foundations. On the other hand, the theoretically sounder theories, e.g. Rice's strain localization criterion [10, 11] have mainly been investigated analytically, for simpler constitutive models and in particular (plane stress or plane strain) loading situations [8, 9, 12, 13, 22].

In this work, a fully three-dimensional framework is set for the application of the Rice's localization criterion, including an advanced, anisotropic elastoplastic constitutive model coupled to a damage model. Both the analytical (for the localization analysis) and algorithmic (for the finite element implementation) moduli are derived in the general case and the model is implemented in the FE code Abaqus/Implicit. Several simple tests are simulated in order to asses the capabilities of this approach.

2 ANISOTROPIC ELASTOPLASTIC MODEL COUPLED WITH DAMAGE

A material description based on rate equations must respect the principle of objectivity. In finite element implementations, the most commonly used technique is to integrate the rate equations in a frame that rotates with the spin **W** (skew-symmetric part of the velocity gradient). This is equivalent to the use of a Jaumann-type stress rate, yet the equations obtained are form-identical to a small strain formulation [18, 24]. Consequently, all the tensor variables below are rotation-compensated with respect to this frame.

This work deals with a general rate-independent, anisotropic, elastoplasticity model, coupled to an isotropic damage model. More precisely, we consider the physically-based hardening model of Teodosiu and Hu [18, 19] and the isotropic damage model of Lemaitre [16]. The coupling is realized through the concept of effective stress:

$$\tilde{\boldsymbol{\sigma}} = \boldsymbol{\sigma}/(1-d) = \mathbf{C} : \boldsymbol{\varepsilon}^e = \mathbf{C} : \left(\boldsymbol{\varepsilon} - \boldsymbol{\varepsilon}^p\right) \tag{1}$$

associated to the principle of strain equivalence [16]. In this equation, d is the continuum damage variable ($d \in [0,1]$, with $d = 0$ for a safe material and $d = 1$ for a completely damaged one). This is a scalar variable thus damage is assumed isotropic, while $\boldsymbol{\sigma}$ is the stress tensor in the damaged material and $\tilde{\boldsymbol{\sigma}}$ is the stress tensor in an equivalent undamaged material. This is the classical framework of continuum damage mechanics.

2.1 Basic equations of the coupled model

The linear elasticity law with damage reads:

$$\boldsymbol{\sigma} = (1-d)\mathbf{C} : \boldsymbol{\varepsilon}^e = (1-d)\mathbf{C} : \left(\boldsymbol{\varepsilon} - \boldsymbol{\varepsilon}^p\right) \tag{2}$$

In rate form, one obtains:

$$\dot{\boldsymbol{\sigma}} = (1-d)\mathbf{C} : \dot{\boldsymbol{\varepsilon}}^e - \dot{d}\mathbf{C} : \boldsymbol{\varepsilon}^e = (1-d)\mathbf{C} : \left(\dot{\boldsymbol{\varepsilon}} - \dot{\boldsymbol{\varepsilon}}^p\right) - \dot{d}\tilde{\boldsymbol{\sigma}} \tag{3}$$

Several possibilities are available for the coupling with a plasticity model [17]. The simplest one is to let damage affect only the stress tensor, while the internal variables describing the hardening remain unaffected. This is the approach used by Lemaitre and co-workers (see [14, 17]) who coupled damage with several isotropic and/or kinematic hardening models. This is the approach used in the current work. It is noteworthy that other authors have proposed models where the other internal variables are also affected by damage [20, 21].

In our case, the yield condition is written in the following form:

$$F = \sqrt{\left(\tilde{\boldsymbol{\sigma}}' - \mathbf{X}\right) : \mathbf{M} : \left(\tilde{\boldsymbol{\sigma}}' - \mathbf{X}\right)} - Y \leq 0 \tag{4}$$

where $\tilde{\boldsymbol{\sigma}}' = \boldsymbol{\sigma}' / \left(1-d\right)$ is the effective deviatoric stress, Y describes the isotropic hardening and $\mathbf{X}$ the kinematic hardening. The associated flow rule reads:

$$\dot{\boldsymbol{\varepsilon}}^p = \dot{\lambda} \frac{\partial F}{\partial \boldsymbol{\sigma}} = \frac{\dot{\lambda}}{\left(1-d\right)} \frac{\mathbf{M} : \left(\tilde{\boldsymbol{\sigma}}' - \mathbf{X}\right)}{\tilde{\bar{\sigma}}} = \frac{\dot{\lambda}}{\left(1-d\right)} \mathbf{V} = \tilde{\mathbf{V}} \dot{\lambda} \tag{5}$$

The rate hardening laws and/or the damage evolution law make use of the equivalent plastic strain rate $\dot{p}$, defined as the power conjugate of the effective equivalent stress $\tilde{\bar{\sigma}}$, i.e.

$$\tilde{\bar{\sigma}} \dot{p} = \left(\tilde{\boldsymbol{\sigma}}' - \mathbf{X}\right) : \dot{\boldsymbol{\varepsilon}}^p \tag{6}$$

The flow rule allows to find a relationship between $\dot{p}$, $\dot{\lambda}$ and d, i.e.

$$\dot{p} = \frac{\dot{\lambda}}{1-d} \tag{7}$$

2.2 Hardening model

The macroscopic hardening models are based on a set of internal variables, describing the isotropic and kinematic hardening. The microstructural hardening model of Teodosiu and Hu is described in detail in [18, 19]. This model makes use of four internal variables: $\mathbf{X}$ and R are the classical back-stress and isotropic hardening variables, while $\mathbf{S}$ is a fourth order tensor describing the directional strength of the planar persistent dislocation structures and $\mathbf{P}$ is a second order dimensionless tensor describing the polarity of these structures. $\mathbf{S}$ is further decomposed along the current plastic strain-rate direction in an active part S_D and a latent part $\mathbf{S}_L$. In general, kinematic hardening models often use the direction $\mathbf{N}$ of plastic strain-rate or the direction $\mathbf{n}$ of deviatoric stress. For a plasticity model coupled to damage, these quantities are defined as:

$$\tilde{\mathbf{N}}\left(d\right) = \frac{\dot{\boldsymbol{\varepsilon}}^p}{\left|\dot{\boldsymbol{\varepsilon}}^p\right|} = \frac{\mathbf{M} : \left(\tilde{\boldsymbol{\sigma}}' - \mathbf{X}\right)}{\left|\mathbf{M} : \left(\tilde{\boldsymbol{\sigma}}' - \mathbf{X}\right)\right|}, \qquad \tilde{\mathbf{n}}\left(d\right) = \frac{\left(\tilde{\boldsymbol{\sigma}}' - \mathbf{X}\right)}{\tilde{\bar{\sigma}}} \tag{8}$$

The model equations are kept identical, except that the directions $\mathbf{N}$ and $\mathbf{n}$ are being replaced by their "effective" counterparts $\tilde{\mathbf{N}}$ and $\tilde{\mathbf{n}}$. The main evolution equations of the Teodosiu model become:

$$\dot{R} = C_R \left(R_{sat} - R\right) \dot{\lambda} = H_R \dot{\lambda} \tag{9}$$

$$\dot{\mathbf{X}} = C_X \left(X_{sat} \tilde{\mathbf{n}} - \mathbf{X}\right) \dot{\lambda} = \mathbf{H}_X \dot{\lambda} \tag{10}$$

$$\dot{S}_D = C_{SD}\left[g\left(S_{sat} - S_D\right) - hS_D\right]\dot{\lambda} = H_{S_D}\dot{\lambda} \tag{11}$$

$$\dot{\mathbf{S}}_L = -C_{SL}\left(\frac{|\mathbf{S}_L|}{S_{sat}}\right)^{n_L}\mathbf{S}_L\dot{\lambda} = \mathbf{H}_{S_L}\dot{\lambda} \tag{12}$$

$$\dot{\mathbf{P}} = C_p\left(\tilde{\mathbf{N}} - \mathbf{P}\right)\dot{\lambda} = \mathbf{H}_P\dot{\lambda} \tag{13}$$

where the decomposition of the $\mathbf{S}$ variable becomes:

$$\mathbf{S} = S_D\tilde{\mathbf{N}}\otimes\tilde{\mathbf{N}} + \mathbf{S}_L \tag{14}$$

Thus, although the coupling with damage modifies the equations, their mathematical structure remains identical to their uncoupled form. This property is very useful for the numerical implementation of the model in a finite element code.

2.3 Damage evolution law

The evolution law of the damage variable d is assumed of the following form [21]:

$$\dot{d} = \begin{cases} \dfrac{1}{(1-d)^{\beta}}\left(\dfrac{Y^e - Y_i^e}{S}\right)^s\dot{\lambda} = H_d\dot{\lambda} & \text{if} \quad Y^e \geq Y_i^e \\ 0 \qquad (\text{i.e.,} \quad H_d = 0) & \text{else} \end{cases} \tag{15}$$

The scalar quantities s, S, β and Y_i^e are material parameters, while $Y^e = \frac{1}{2}\boldsymbol{\varepsilon}^e : \mathbf{C} : \boldsymbol{\varepsilon}^e$ is the elastic strain energy release rate:

$$Y^e = \frac{J_2^{\,2}}{2E}\left[\frac{2}{3}(1+\nu) + 3(1-2\nu)\left(\frac{\tilde{\sigma}^s}{J_2}\right)^2\right] \tag{16}$$

where $\tilde{\sigma}^s = \frac{1}{3}tr(\tilde{\boldsymbol{\sigma}})$ is the effective hydrostatic stress, while $J_2 = \sqrt{\frac{3}{2}\tilde{\boldsymbol{\sigma}}' : \tilde{\boldsymbol{\sigma}}'}$ is the effective von Mises equivalent stress.

2.4 Analytical tangent modulus

Rate-independent elastoplastic laws can be written in the following compact form:

$$\dot{\boldsymbol{\sigma}} = \mathbf{L}^{ana} : \dot{\boldsymbol{\varepsilon}} \tag{17}$$

where $\mathbf{L}^{ana}$ is the so-called analytical tangent modulus. The expression of this modulus is required for the application of the localization criterion of Rice to the chosen material.

Let us first determine the plastic multiplier $\dot{\lambda}$. The consistency condition $\dot{F} = 0$ leads to:

$$\dot{\tilde{\bar{\sigma}}} - \dot{Y} = 0 \tag{18}$$

The first term is obtained by the chain rule as:

$$\dot{\tilde{\bar{\sigma}}} = \frac{\partial\tilde{\bar{\sigma}}}{\partial\tilde{\boldsymbol{\sigma}}'} : \dot{\tilde{\boldsymbol{\sigma}}}' + \frac{\partial\tilde{\bar{\sigma}}}{\partial\mathbf{X}} : \dot{\mathbf{X}} = \frac{\partial\tilde{\bar{\sigma}}}{\partial\tilde{\boldsymbol{\sigma}}'} : \left(\dot{\tilde{\boldsymbol{\sigma}}}' - \dot{\mathbf{X}}\right) \tag{19}$$

and its subsequent terms are obtained as follows:

$$\dot{\tilde{\boldsymbol{\sigma}}}' = \mathbf{C} : \left(\dot{\boldsymbol{\varepsilon}}' - \dot{\boldsymbol{\varepsilon}}^p\right) = \mathbf{C} : \left(\dot{\boldsymbol{\varepsilon}}' - \tilde{\mathbf{V}}\dot{\lambda}\right) \tag{20}$$

$$\frac{\partial \tilde{\bar{\sigma}}}{\partial \tilde{\boldsymbol{\sigma}}'} = \frac{\mathbf{M} : (\tilde{\boldsymbol{\sigma}}' - \mathbf{X})}{\tilde{\bar{\sigma}}} = \mathbf{V} \tag{21}$$

$$\dot{\mathbf{X}} = \mathbf{H}_X \dot{\lambda} \tag{22}$$

$$\dot{Y} = H_Y \dot{\lambda} \tag{23}$$

Back-substituting these results leads to the following expression for the plastic multiplier:

$$\dot{\lambda} = \frac{\mathbf{V} : \mathbf{C} : \dot{\boldsymbol{\varepsilon}}'}{H_\lambda} = \frac{\mathbf{V} : \mathbf{C} : \dot{\boldsymbol{\varepsilon}}}{H_\lambda} \tag{24}$$

where H_λ is the scalar hardening modulus, affected by damage:

$$H_\lambda = \mathbf{V} : \mathbf{C} : \tilde{\mathbf{V}} + \mathbf{V} : \mathbf{H}_X + H_Y \tag{25}$$

Finally, after replacement in Eq. (3) and rearrangements of terms, the following linear relationship is found:

$$\dot{\boldsymbol{\sigma}} = \left[\tilde{\mathbf{C}} - \alpha \left(\frac{(\tilde{\mathbf{C}} : \tilde{\mathbf{V}}) \otimes (\mathbf{V} : \mathbf{C})}{H_\lambda} + \frac{H_d \tilde{\boldsymbol{\sigma}} \otimes (\mathbf{V} : \mathbf{C})}{H_\lambda} \right) \right] : \dot{\boldsymbol{\varepsilon}} \tag{26}$$

where $\alpha = 1$ for elastoplastic loading and 0 otherwise, and $\tilde{\mathbf{C}} = (1-d)\mathbf{C}$.

If there is no damage in the model, then $\tilde{\mathbf{C}} = \mathbf{C}$, $\tilde{\mathbf{V}} = \mathbf{V}$, $\tilde{\boldsymbol{\sigma}} = \boldsymbol{\sigma}$ and H_d vanishes; in this case, it is easy to see that the classical expression of the elastoplastic tangent modulus is recovered (see e.g. [23]).

3 NUMERICAL IMPLEMENTATION

In a finite element code, the constitutive model takes the form of a stress (and state) update scheme between a time t (at time step n) and the subsequent time $t+\Delta t$ (increment $n+1$). The numerical implementation of the model is done here using an implicit time integration scheme. An accurate, implicit state update algorithm has been developed for the elastoplasticity model [23]. The numerical implementation for the damage-coupled model will follow the same approach and, under some assumptions, it will take a very similar form.

First, the discrete forms of the constitutive equations are reviewed. Then, the main steps for the calculation of the algorithmic tangent modulus are given.

3.1 Discrete form of the constitutive equations

Elasticity and normality laws. The discrete form of the elasticity law is:

$$\Delta \tilde{\boldsymbol{\sigma}} = \mathbf{C} : \Delta \boldsymbol{\varepsilon}^e = \mathbf{C} : \left(\Delta \boldsymbol{\varepsilon} - \Delta \boldsymbol{\varepsilon}^p \right) \tag{27}$$

This leads to the stress update equation:

$$\boldsymbol{\sigma}_{n+1} = (1 - d_{n+1}) \left[\tilde{\boldsymbol{\sigma}}_n + \mathbf{C} : \left(\Delta \boldsymbol{\varepsilon} - \Delta \boldsymbol{\varepsilon}^p \right) \right] \tag{28}$$

where $\tilde{\boldsymbol{\sigma}}_n = \boldsymbol{\sigma}_n / (1 - d_n)$. It appears that the final stress depends both on plastic strain and damage. The plastic strain increment is obtained from the discrete normality rule:

$$\Delta\boldsymbol{\varepsilon}^{p} = \Delta\lambda \left.\frac{\partial F}{\partial \boldsymbol{\sigma}}\right|_{n+1} = \frac{1}{1-d_{n+1}} \mathbf{V}_{n+1} \Delta\lambda = \tilde{\mathbf{V}}_{n+1} \Delta\lambda \tag{29}$$

where the implicit character of the scheme clearly appears.

Hardening variables. The hardening variables are governed by rate equations having the form $\dot{\mathbf{y}} = \mathbf{H}_{\mathrm{y}} \dot{\lambda}$. According to [23], they are updated with an implicit, semi-analytical scheme. The following update equations are obtained in the form:

$$\mathbf{y}_{n+1} = \mathbf{y}_{n} + \Delta\mathbf{y}\left(\boldsymbol{\sigma}_{n+1,} \mathbf{y}_{n+1}, \Delta\lambda, d_{n+1}\right) \tag{30}$$

Damage. The same semi-analytical time integration approach is used for the damage variable as in [23]:

$$\begin{aligned} d_{n+1} &= 1 - \left[\left(1-d_{n}\right)^{1+\beta} - \left(1+\beta\right)\left(\frac{Y^{e}{}_{n+1} - Y_{i}^{e}}{S} \right)^{S} \Delta\lambda \right]^{\frac{1}{1+\beta}} && \text{if } Y^{e}{}_{n+1} \geq Y_{i}^{e} \\ d_{n+1} &= d_{n} && \text{otherwise} \end{aligned} \tag{31}$$

3.2 Numerical resolution

The resolution of the previous set of nonlinear equations is made by a Newton-Raphson procedure. In [23], the equations of the elastoplastic model have been reduced to a set of two equations, with the main variables $\mathbf{T}$ and $\Delta\lambda$. The size-reduction is a common preoccupation when constitutive models are implemented (see e.g. [21, 23, 25] etc.). This approach ensures the robustness of the Newton-Raphson resolution. In the case of the damage-coupled model, this two-equation system is written as:

$$\begin{bmatrix} \tilde{\mathbf{T}}_{n+1} - \tilde{\mathbf{T}}_{n} - 2G\Delta\boldsymbol{\varepsilon}' + 2G\Delta\lambda\tilde{\mathbf{V}}\left(\tilde{\mathbf{T}}_{n+1}\right) + \Delta\mathbf{X}\left(\tilde{\mathbf{T}}_{n+1}, \Delta\lambda\right) \\ \tilde{\bar{\sigma}}\left(\tilde{\mathbf{T}}_{n+1}\right) - Y\left(\Delta\lambda\right) \end{bmatrix} = \begin{bmatrix} \mathbf{0} \\ 0 \end{bmatrix} \tag{32}$$

where $\tilde{\mathbf{T}} = \tilde{\boldsymbol{\sigma}}' - \mathbf{X}$. Nevertheless, this system is underdetermined since the unknowns are now $\tilde{\mathbf{T}}_{n+1}$, $\Delta\lambda$ but also d_{n+1}. A third equation should be added to the system and then the new system could be solved for a fully implicit solution. For the current implementation, a simpler approach has been chosen. The damage equation is uncoupled at every increment, from this system, by considering the value d_{n} instead of d_{n+1} wherever it explicitly appears in system (32). By doing this, the numerical resolution becomes very similar to the one for undamaged model. It should be noted that the damage equation exhibits a yield value, thus during an important part of the loading history the previous approximation will have no impact on the solution. During the last part, when damage is activated, the strain increments should be kept restricted to safe values, in order to ensure the overall accuracy.

3.3 Consistent tangent modulus

For the finite element equilibrium resolution, the constitutive algorithm must also provide the variation of the stress increment due to a variation in the strain increment:

$$D\Delta\boldsymbol{\sigma} = \mathbf{L}^{a\mathrm{lg}} : D\Delta\boldsymbol{\varepsilon} \tag{33}$$

The fourth-order tensor $\mathbf{L}^{alg}$ is the so-called consistent tangent modulus, which we shall calculate hereafter. The differentiation of the elasticity law gives:

$$D\Delta\boldsymbol{\sigma} = (1-d)\mathbf{C} : D\Delta\boldsymbol{\varepsilon} - (1-d)2GD\Delta\boldsymbol{\varepsilon}^{p} - \tilde{\boldsymbol{\sigma}}Dd \tag{34}$$

The normality rule yields a linear relationship between $D\Delta\boldsymbol{\varepsilon}^{p}$ and $D\Delta\boldsymbol{\varepsilon}$ while the yield condition gives a relationship between $\Delta\lambda$ and $D\Delta\boldsymbol{\varepsilon}$:

$$D\Delta\boldsymbol{\varepsilon}^{p} = \Delta\lambda D\tilde{\mathbf{V}} + \tilde{\mathbf{V}}D\Delta\lambda \tag{35}$$

The differentiation of the yield criterion and $\tilde{\mathbf{V}}$ respectively, gives:

$$D\Delta\lambda = \frac{\mathbf{V}}{H} : D\tilde{\mathbf{T}} \tag{36}$$

$$D\tilde{\mathbf{V}} = \tilde{\mathbf{Q}} : D\tilde{\mathbf{T}} + \frac{1}{1-d}\tilde{\mathbf{V}}Dd \tag{37}$$

where:

$$\tilde{\mathbf{Q}} = \frac{\partial\tilde{\mathbf{V}}}{\partial\tilde{\mathbf{T}}} = \frac{1}{(1-d)\tilde{\bar{\sigma}}}(\mathbf{M} - \mathbf{V}\otimes\mathbf{V}), \qquad H = \frac{\partial Y}{\partial\Delta\lambda} \tag{38}$$

By replacing $D\Delta\lambda$ and $D\tilde{\mathbf{V}}$ in Eq. (35) and then in Eq. (34), one can obtain:

$$D\Delta\boldsymbol{\sigma} = (1-d)\mathbf{C} : D\Delta\boldsymbol{\varepsilon} - (1-d)2G\left(\Delta\lambda\tilde{\mathbf{Q}} + \frac{\tilde{\mathbf{V}}\otimes\mathbf{V}}{H}\right) : D\tilde{\mathbf{T}} - \left(\tilde{\boldsymbol{\sigma}} + 2G\Delta\lambda\tilde{\mathbf{V}}\right)Dd \tag{39}$$

One still has to express $D\tilde{\mathbf{T}} = D\tilde{\boldsymbol{\sigma}}' - D\mathbf{X}$. By differentiating $\tilde{\boldsymbol{\sigma}}'$ and $\mathbf{X}$, and replacing in the relation of $D\tilde{\mathbf{T}}$, one can obtain:

$$D\tilde{\mathbf{T}} = 2G\boldsymbol{\Lambda}^{-1} : D\Delta\boldsymbol{\varepsilon}' = 2G\boldsymbol{\Lambda}^{-1} : D\Delta\boldsymbol{\varepsilon} \tag{40}$$

where:

$$\boldsymbol{\Lambda} = \mathbf{I}_4' + 2G\left(\Delta\lambda\tilde{\mathbf{Q}} + \tilde{\mathbf{V}}\otimes\frac{\mathbf{V}}{H}\right) + \frac{\partial\mathbf{X}}{\partial\tilde{\mathbf{T}}} + \left(\frac{1}{H}\frac{\partial\mathbf{X}}{\partial\Delta\lambda} + \frac{2G\Delta\lambda}{H}\frac{1}{1-d}\frac{\partial d}{\partial\Delta\lambda}\tilde{\mathbf{V}}\right)\otimes\mathbf{V} \tag{41}$$

Also, Dd reads:

$$Dd = \frac{2G}{H}\frac{\partial d}{\partial\Delta\lambda}\left(\mathbf{V} : \boldsymbol{\Lambda}^{-1}\right) : D\Delta\boldsymbol{\varepsilon} \tag{42}$$

By replacing all terms, $D\Delta\boldsymbol{\sigma}$ can be linearly related to $D\Delta\boldsymbol{\varepsilon}$ (see Eq. (33)) using the consistent modulus $\mathbf{L}^{alg}$ which takes the form:

$$\mathbf{L}^{alg} = (1-d)\mathbf{C} - (1-d)4G^{2}\left(\Delta\lambda\tilde{\mathbf{Q}} + \frac{\tilde{\mathbf{V}}\otimes\mathbf{V}}{H}\right) : \boldsymbol{\Lambda}^{-1} - \frac{2G}{H}\frac{\partial d}{\partial\Delta\lambda}\left(\tilde{\boldsymbol{\sigma}} + 2G\Delta\lambda\tilde{\mathbf{V}}\right)\otimes\left(\mathbf{V} : \boldsymbol{\Lambda}^{-1}\right) \tag{43}$$

This last equation defines the algorithmic modulus $\mathbf{L}^{alg}$ to be used for the numerical implementation in a finite element code.

4 LOCALISATION CRITERION

In this work, we focus on the localization criterion proposed by Rice [6-11, 15]. We shall briefly recall the basic ideas of this criterion and then calculate the particular form of the analytical tangent modulus required for its application.

4.1 Rice's localization criterion

This criterion applies to a continuous medium subjected to a homogeneous strain state. The strain localization is searched as a bifurcation phenomenon, meaning that a non-homogeneous straining mode becomes possible (the uniqueness of the solution is lost). This non-homogeneity is considered as a planar localization band, defined by its normal $\mathbf{n}$. The velocity gradient inside and outside the band are respectively denoted $\mathbf{G}^-$ and $\mathbf{G}^+$ while the corresponding nominal stresses are denoted $\mathbf{N}^-$ and $\mathbf{N}^+$. The nominal stress rate is related to the velocity gradient by the following constitutive law:

$$\dot{\mathbf{N}} = \mathfrak{J} : \mathbf{G} \tag{44}$$

where $\mathfrak{J}$ is an analytical tangent modulus that has to be expressed in terms of $\mathbf{L}^{ana}$. The continuity of the stress vector through the band of normal $\mathbf{n}$ is written:

$$\mathbf{n}.\left[\dot{\mathbf{N}}\right] = 0 \tag{45}$$

where $\left[\mathbf{A}\right] = \mathbf{A}^+ - \mathbf{A}^-$ designates the jump in a quantity $\mathbf{A}$ across the chosen plane. Hadamard's equation of compatibility for the velocity field states that a vector $\boldsymbol{\lambda}$ exists such that the jump in $\mathbf{G}$ reads:

$$\left[\mathbf{G}\right] = \boldsymbol{\lambda} \otimes \mathbf{n} \tag{46}$$

Thus $\boldsymbol{\lambda} = \mathbf{0}$ enforces a continuous velocity field. Combining Eqs. (44)-(46), one obtains:

$$\left\{\mathbf{n}.\mathfrak{J}.\mathbf{n}\right\}.\boldsymbol{\lambda} = \mathbf{0} \tag{47}$$

This is a typical eigenvalue problem and a nontrivial solution for $\boldsymbol{\lambda}$ (i.e., bifurcation condition $\boldsymbol{\lambda} \neq \mathbf{0}$) requires the vanishing of the following determinant:

$$\det\left\{\mathbf{n}.\mathfrak{J}.\mathbf{n}\right\} = 0 \tag{48}$$

This last equation gives a necessary condition for a localization band to appear; it describes the strain localization criterion introduced by Rice.

4.2 Tangent modulus for the localization criterion

The application of the former localization criterion requires the calculation of the modulus $\mathfrak{J}$. In a fixed frame, the linear hypo-elasticity law reads:

$$\overset{\circ}{\tilde{\boldsymbol{\sigma}}} = \mathbf{C} : \left(\mathbf{D} - \mathbf{D}^p\right) \tag{49}$$

where $\overset{\circ}{\tilde{\boldsymbol{\sigma}}}$ designates the Jaumann derivative of the effective Cauchy stress:

$$\overset{\circ}{\tilde{\boldsymbol{\sigma}}} = \dot{\tilde{\boldsymbol{\sigma}}} - \mathbf{W}.\tilde{\boldsymbol{\sigma}} + \tilde{\boldsymbol{\sigma}}.\mathbf{W} \tag{50}$$

The stress rate can be thus expressed as:

$$\dot{\boldsymbol{\sigma}} = (1-d)\,\overset{\circ}{\tilde{\boldsymbol{\sigma}}} - \dot{d}\tilde{\boldsymbol{\sigma}} + \mathbf{W}.\boldsymbol{\sigma} - \boldsymbol{\sigma}.\mathbf{W} \tag{51}$$

The Cauchy stress and the nominal stress are related to each other by the classical relation:

$$J\boldsymbol{\sigma} = \mathbf{F}.\mathbf{N} \tag{52}$$

where $\mathbf{F}$ is the deformation gradient and $J = \det(\mathbf{F})$ its jacobian. Thus:

$$\dot{\mathbf{N}} = J\mathbf{F}^{-1}.\left(\boldsymbol{\sigma}\ tr(\mathbf{D}) + \dot{\boldsymbol{\sigma}} - \mathbf{G}.\boldsymbol{\sigma}\right) \tag{53}$$

In an updated lagrangian formulation, $\mathbf{F} = \mathbf{I}$ and $J = 1$; Eq. (53) simplifies as:

$$\dot{\mathbf{N}} = \dot{\boldsymbol{\sigma}} + \boldsymbol{\sigma}\ tr(\mathbf{D}) - \mathbf{G}.\boldsymbol{\sigma} \tag{54}$$

and, replacing the Cauchy stress rate from Eq. (51):

$$\dot{\mathbf{N}} = (1-d)\mathbf{C} : \left(\mathbf{D} - \mathbf{D}^{p}\right) - \dot{d}\tilde{\boldsymbol{\sigma}} - \boldsymbol{\sigma}.\mathbf{W} + \boldsymbol{\sigma}\ tr(\mathbf{D}) - \mathbf{D}.\boldsymbol{\sigma} \tag{55}$$

All terms on the right-hand side of this expression can be linearly expressed in terms of the velocity gradient **G**, in the following way:

$$(1-d)\mathbf{C} : \left(\mathbf{D} - \mathbf{D}^{p}\right) - \dot{d}\tilde{\boldsymbol{\sigma}} = \mathbf{L}^{ana} : \mathbf{G} \tag{56}$$

$$\boldsymbol{\sigma}\ tr(\mathbf{D}) = \mathbf{A}_1 : \mathbf{G} \tag{57}$$

$$\mathbf{D}.\boldsymbol{\sigma} = \mathbf{A}_2 : \mathbf{D} = \mathbf{A}_2 : \mathbf{G} \tag{58}$$

$$\boldsymbol{\sigma}.\mathbf{W} = \mathbf{A}_3 : \mathbf{G} \tag{59}$$

where $\mathbf{L}^{ana}$ is the analytical tangent modulus from Eqs. (17) and (26), while $\mathbf{A}_1$, $\mathbf{A}_2$ and $\mathbf{A}_3$ are fourth order tensors that can be expressed, after some mathematical manipulations, as:

$$A_{1ijkl} = \sigma_{ij}\delta_{kl} \tag{60}$$

$$A_{2ijkl} = \tfrac{1}{2}\left[\delta_{ik}\sigma_{lj} + \delta_{il}\sigma_{kj}\right] \tag{61}$$

$$A_{3ijkl} = \tfrac{1}{2}\left[\sigma_{ik}\delta_{lj} - \sigma_{il}\delta_{jk}\right] \tag{62}$$

$$\mathfrak{I} = \mathbf{L}^{ana} + \mathbf{A}_1 - \mathbf{A}_2 - \mathbf{A}_3 \tag{63}$$

It is noteworthy that $\mathfrak{I}$ possesses no symmetry, due to the particular forms of the three $\mathbf{A}_i$ terms.

5 NUMERICAL RESULTS

For the investigation of the selected strain localization criterion, several simple loadings are considered. They are very regular in-plane loading cases for sheet metal rheological testing, while they are also used for the experimental and numerical assessment of the forming limit diagram, using various models. In the principal stress frame, we shall consider the two principal stresses in directions 1 and 2, with $\sigma_{11}>\sigma_{22}$, while $\sigma_{33}=0$ for all tests (see Figure 1). Nevertheless, the calculations are fully three-dimensional, which is different from most of the results available in the literature. Three monotonous tests are selected: uniaxial tensile test, plane strain tensile test and simple shear test.

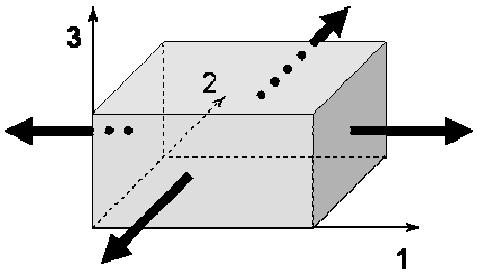

Figure 1: Loading imposed to a material volume during the selected tests. Stress principal frame.

Typical material parameters for mild steel have been selected. The stress-strain curves corresponding to three monotonous tests are represented in Figure 2 (thick lines). Moreover, two sequential tests are represented in the same figure (thin lines). They represent the typical reverse and orthogonal strain-path changes. The main features of the Teodosiu-Hu hardening model (see e.g. [19]) when strain-path changes occur are clearly reproduced. On the other side, the coupling with the damage model introduces a softening behavior.

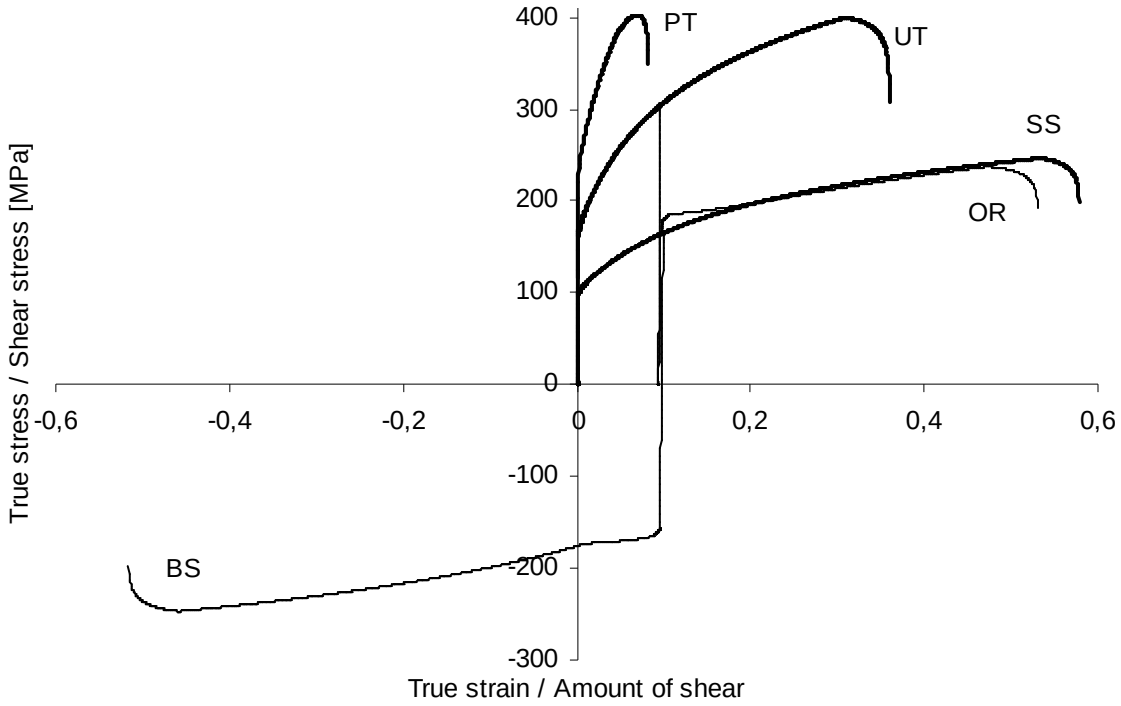

Figure 2: Prediction of simple rheological tests using the coupled model: Hill quadratic yield surface, Teodosiu-Hu hardening model and Lemaitre damage model.
UT = uniaxial tensile test; plot: σ_{11} vs. ε_{11}.
PT = plane strain tensile test; plot: σ_{11} vs. ε_{11}.
SS = simple shear test; plot: σ_{12} vs. ε_{12}.
BS = simple shear + reverse shear (Bauschinger) test; plot: σ_{12} vs. ε_{12}.
OR = uniaxial tension + simple shear (orthogonal) test; plot: σ_{11} vs. ε_{11}, then σ_{12} vs. ε_{12}.

In the case of a simpler, von Mises plasticity model, the three tests are characterized by the strain ratios given in table 1. This particular case allows us to compare our results to data available in literature [22]. For the strain analysis at localization, the corresponding principal

strains for these three monotonous tests are plotted in Figure 3. Again, this result corresponds to the typical forming limit diagrams obtained experimentally in sheet metal testing. It is also noteworthy that the value of damage when localization occurs is not the same for the three tests.

Test	$\varepsilon_2/\varepsilon_1$
Simple shear test	-1
Uniaxial tensile test	-1/2
Plane strain tensile test	0

Table 1: Strain ratios for the three monotonous tests.

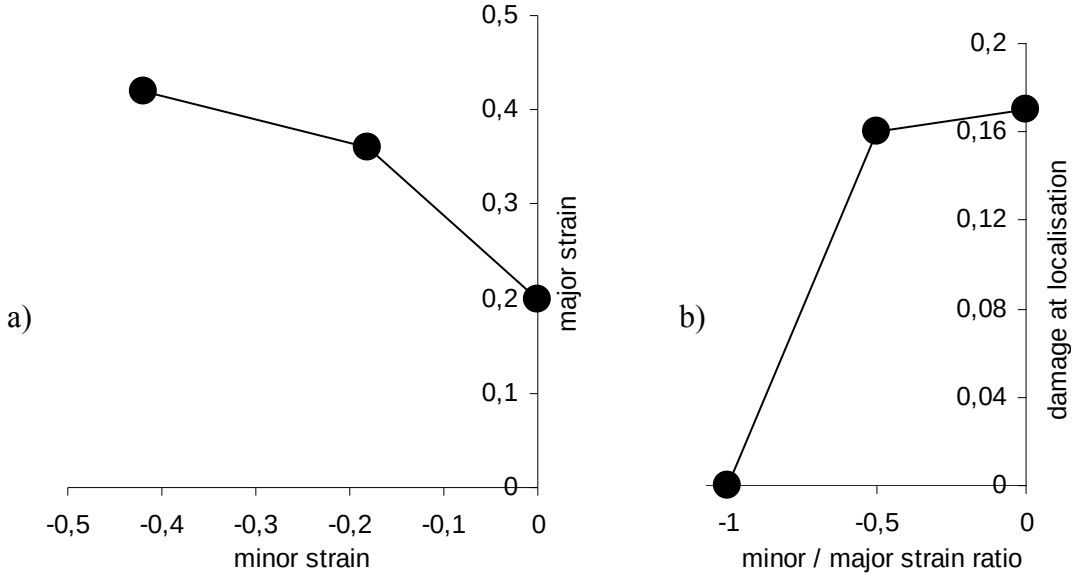

Figure 3: a) Limit strains for the three monotonous tests. From left to right: simple shear, uniaxial tension and plane strain tension. b) Limit values of damage at localization.

The Rice's localization criterion also provides the orientation of the localization band. This orientation can be defined by two angles, as shown in Figure 4a: the angle θ_1 gives the inclination of the band with respect to axis 1 in the plane 1-2, while the angle θ_2 gives the inclination of the band with respect to axis 3, in a plane perpendicular to the band. For sheet materials, these two angles correspond to the in-plane orientation of the band, as well as its out-of-plane inclination. Many analytical developments available in literature assume that this last angle vanishes.

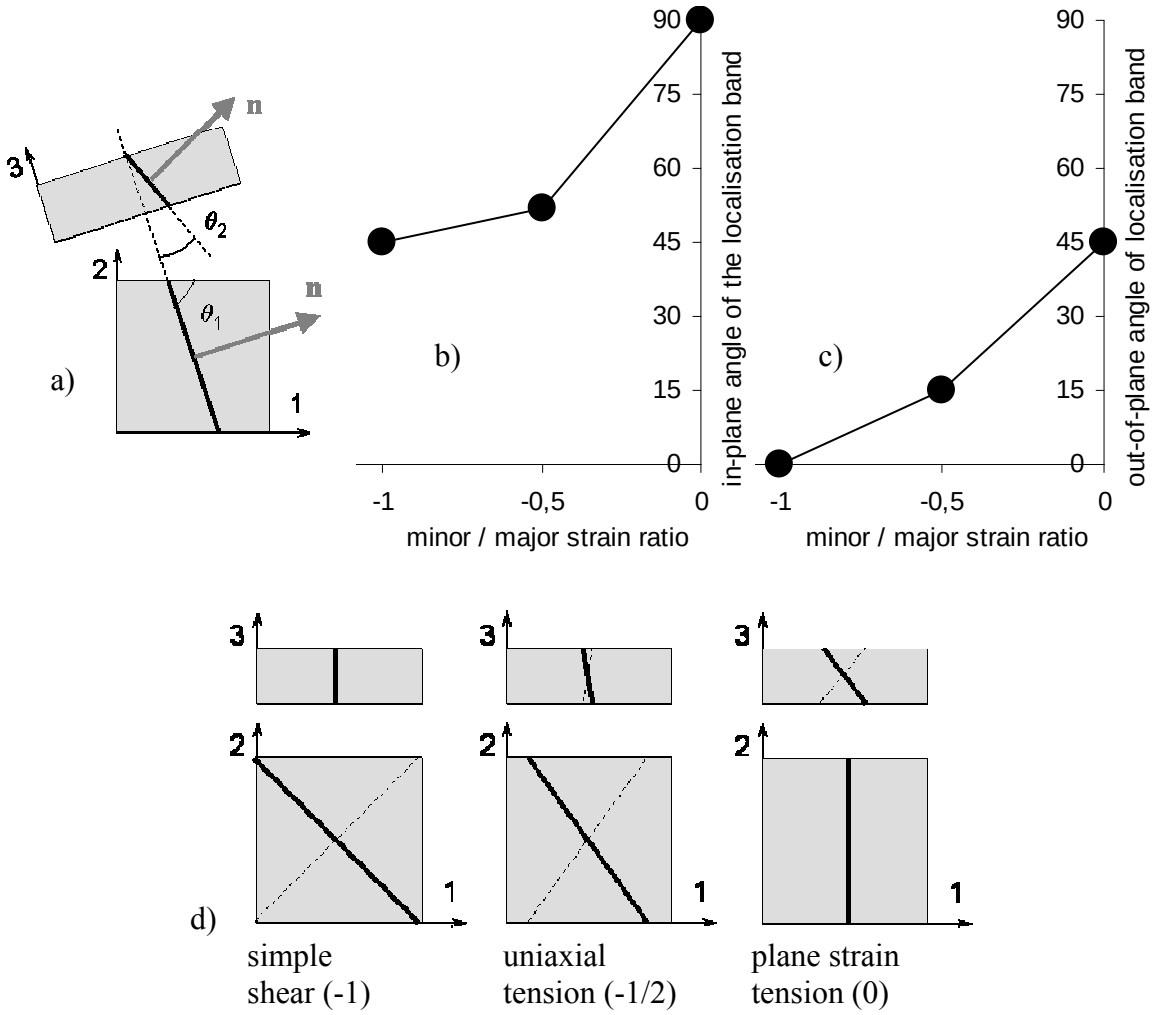

Figure 4: Orientation of the localization band: a) definition of the orientation with two angles, b) values of the in-plane and c) of the out-of-plane angles d) graphical representation of the localization band orientation (dotted lines represent the other possible orientations).

The values of the in-plane angle for simple shear and uniaxial tension correspond to both the experimental values as well as those predicted with other models. For the plane strain tension, our result corresponds precisely to the experimental observations, as well as the prediction of the Marciniak-Kuczynski model. Analytical calculations using the Rice model, where the normal to the localization band is considered in the 1-2 plane (see e.g. [22]) predict an in-plane angle close, yet smaller than 90°. A possible explanation for this discrepancy may be due to the out-of-plane inclination of the localization band in the three-dimensional analysis. As one can see in Figure 4c, this angle is zero for simple shear, quite small for uniaxial tension, while it reaches 45° for the plane strain tensile test. Although the analysis is purely theoretical, the graphical representations from Figure 4d clearly correspond to the experimental localization modes for the considered tests.

6 CONCLUSIONS

In this work, an advanced anisotropic elastoplastic model has been coupled to an isotropic damage model and accurately implemented in a finite element code. The bifurcation condition of Rice has been applied as a localization criterion for this material model. For this purpose,

various forms of analytical and algorithmic tangent moduli have been developed in a general, fully three-dimensional framework. The orientation of the planar band of localization has also been searched for, in the whole space of possible orientations.

Simple mechanical tests have been simulated. These first numerical applications reproduce the experimental trends both in terms of limit strains and localization band orientation. The possibility of out-of-plane directions of the localization plane has proven necessary and allowed for interesting and original results.

The modeling framework will thus be further generalized to more complex damage models and their numerical implementation in a fully implicit way. The model can be applied for the prediction of linear and nonlinear forming limit diagrams, as well as strain localization predictions in finite element simulations of forming processes.

REFERENCES

[1] S.P. Keeler, Determination of the forming limits in automotive stamping, Sheet Metal Industr. 42, 683–703, 1965.

[2] A. Considère, Mémoire sur l'emploi du fer et de l'acier dans les constructions, Annales des Ponts et Chaussées, 9, 574, 1885.

[3] W. Swift, Plastic instability under plane stress, J. Mech. Phys. Solids 1, 1–18, 1952.

[4] R. Hill, A general theory of uniqueness and stability in elastic–plastic solids, J. Mech. Phys. Solids, 6, 236–249, 1958.

[5] Z. Marciniak, K. Kuczynski, Limit strains in the process of stretch forming sheet metal, Int. J. Mech. Sci., 9, 609–620, 1967.

[6] M. Habbad, Instabilités plastiques en élastoplasticité anisotrope en grandes déformations. PHD Thesis, Ecole centrale de Lyon, 1994.

[7] G. Barbier, A. Benallal, V. Cano, Relation théorique entre la méthode de perturbation linéaire et l'analyse de bifurcation pour la prédiction de la localisation des déformations. C. R. Acad. Sci. Paris, 1998.

[8] A. Benallal, C. Comi, On localization in saturated porous continua. C. R. Acad. Sci. Paris, 2000.

[9] A. Benallal, D. Bigoni, Effects of temperature and termo-mechanical couplings on material instabilities and strain localization of inelastic materials. Journal of the Mechanics and Physics of Solids, 2003.

[10] J.R. Rice, The localization of plastic deformation. Theoretical and Applied Mechanics, 1976.

[11] J.W. Rudnicki, J.R. Rice, Conditions for the localization of deformation in pressure-sensitive dilatant materials. J. Mech. Phys. Solids, 1975.

[12] D. Bigoni, T. Hueckel, Uniqueness and localization-Part I: Associative and non-associative elastoplasticity. International Journal of Solids and Structures, 1990.

[13] D. Bigoni, T. Hueckel, Uniqueness and localization-Part II: Coupled elastoplasticity. International Journal of Solids and Structures, 1990.

[14] J. Lemaitre, R. Desmorat, M. Sauzay, Anisotropic damage law of evolution. Eur. J. Mech., 1999.

[15] V. Keryvin, Contribution à la modélisation de l'endommagement localisé. PhD Thesis, Université de Poitiers, 1999.

[16] J. Lemaitre, J.L. Chaboche, Mécanique des matériaux solides. Editions Dunod, Paris, 1986.

[17] J.L. Chaboche, Thermodynamically founded CDM models for creep and other conditions: CISM Courses and lectures No.399, International Centre for Mechanical Sciences. Creep and Damage in Materials and structures, 209-283, 1999.

[18] C. Teodosiu, Z. Hu, Evolution of the intragranular microstructure at moderate and large strains: Modeling and computational significance. Shen & Dawson editors, Simulation of Material Processing: Theory, Methods and Applications, 173-182, 1995.

[19] C. Teodosiu, Z. Hu, Microstructure in the continuum modeling of plastic anisotropy. In: 19th Riso International Symposium on Materials Science Proceedings, Roskilde, 149-168, 1998.

[20] A. Cherouat, K. Saanouni, Y. Hammi, Improvement of forging process of a 3D complex part with respect to damage occurrence. Journal of Materials processing Technology 142, 307-317, 2003.

[21] M. Khelifa, Simulation numérique de l'endommagement en formage des structures minces. PhD Thesis, Université de Technologie de Troyes, 2004.

[22] I. Doghri, R. Billardon, Investigation of localization due to damage in elasto-plastic materials. Mechanics of Materials 19, 129-149, 1995.

[23] B. Haddag, T. Balan, F. Abed-Meraim, Investigation of advanced strain-path dependent material models for sheet metal forming simulations. Int. J. Plasticity, to appear, 2006.

[24] T.J.R. Hughes, J. Winget, Finite rotation effects in numerical integration of rate constitutive equation arising in large deformation analysis. Int. J. Num. Methods Engng. 15:12 (1980) 1862-1867.

[25] J.L. Alves, Simulação numérica do processo de estampagem de chapas metálicas: Modelação mecânica e métodos numéricos. Ph. D. Thesis, University of Minho, Portugal. 2003.